Electronic structure for the series of Cu based chalcopyrites of the CuInM$_2^{VI}$ type

H. Tototzintle-Huitle[a,b], J.A. Rodríguez[c], and R. Baquero[a]
[a]*Department of Physics, Centro de Investigación y de Estudios Avanzados del IPN, Apartado Postal 14-740, 07000 México D.F.,*
[b]*Centro de Investigación y de Estudios Avanzados del IPN, Unidad Querétaro, Apartado Postal 1-798, Querétaro, Qro. 76001 México,*
[c]*Department of Physics, Universidad Nacional de Colombia, Ciudad Universitaria, Bogotá, Colombia.*

Recibido el 18 de octubre de 2007; aceptado el 27 de noviembre de 2007

In this paper we study the electronic band structure for the series of Cu-based chalcopyrites CuInM$_2^{VI}$ with M^{VI}= S,Se,Te. We use the tight-binding method and obtain the tight-binding parameters in such a way that we fit the experimental gap value for the whole series of Cu-based chalcopyrites. Chalcopyrites can deviate from the ideal symmetry in two ways: tetragonal deformation and anionic distortion. In this paper, we calculate the ideal configuration and the effect of anionic distortion. Our calculation can be used further to obtain surface, interface and superlattice electronic band structures using the Surface Green's Function Matching Method in a straightforward way.

Keywords: Electronic structure; chalcopyrites; anionic distortion.

Estudiamos la estructura electrónica de bandas para la serie de calcopiritas basadas en Cu del tipo CuInM$_2^{VI}$ donde M=S, Se, Te. Usamos el método de amarre fuerte y obtenemos los parámetros de amarre fuerte de tal manera que obtenemos el valor de la brecha óptica experimental para toda la serie de calcopiritas basadas en Cu. Las calcopiritas se pueden desviar de la simetría ideal en dos formas. La deformación tetragonal y la deformación aniónica. En este trabajo calculamos la configuración ideal y el efecto de la distorsión aniónica. Nuestros cálculos pueden ser utilizados para obtener la estructura de bandas de superficies, interfaces y superredes usando el método de acoplamiento de las funciones de Green de superficie de una manera directa.

Descriptores: Estructura electrónica; calcopiritas; distorsión aniónica.

PACS: 71.20.-b; 71.20.Nr; 73.20.At

1. Introduction

The quest for room temperature ferromagnetic semiconductors that can be matched to conventional semiconductors resulted in an increasing interest in A^{II}B^{IV}M$_2^V$ as well as in A^{I}B^{III}M$_2^{VI}$ chalcopyrites [1]. These materials are also interesting as non-linear optical devices [2, 3], in chemisorption [4] and in solar cell applications with a high efficiency-to-cost ratio [5–7].

Chalcopyrites are tetragonal centered crystallographic structures with eight atoms in the unit cell basis. Their spatial group is the D_{2d}^{12}. In Fig. 1 we present their crystal structure, and the location and identification of the eight atoms in the CuInM$_2^{VI}$ unit cell is shown in Table I.

TABLE I. Positions of the atoms in the unit cell in the ideal case.

No.	atom	ideal
1	In	$(0,0,0)$
2	C^{VI}	$\left(\frac{1}{4},\frac{1}{4},\frac{1}{8}\right)$
3	Cu	$\left(\frac{1}{2},0,\frac{1}{4}\right)$
4	C^{VI}	$\left(\frac{3}{4},\frac{1}{4},\frac{3}{8}\right)$
5	Cu	$\left(0,0,\frac{1}{2}\right)$
6	C^{VI}	$\left(\frac{1}{4},\frac{1}{4},\frac{5}{8}\right)$
7	In	$\left(\frac{1}{2},0,\frac{3}{4}\right)$
8	C^{VI}	$\left(\frac{3}{4},\frac{1}{4},\frac{7}{8}\right)$

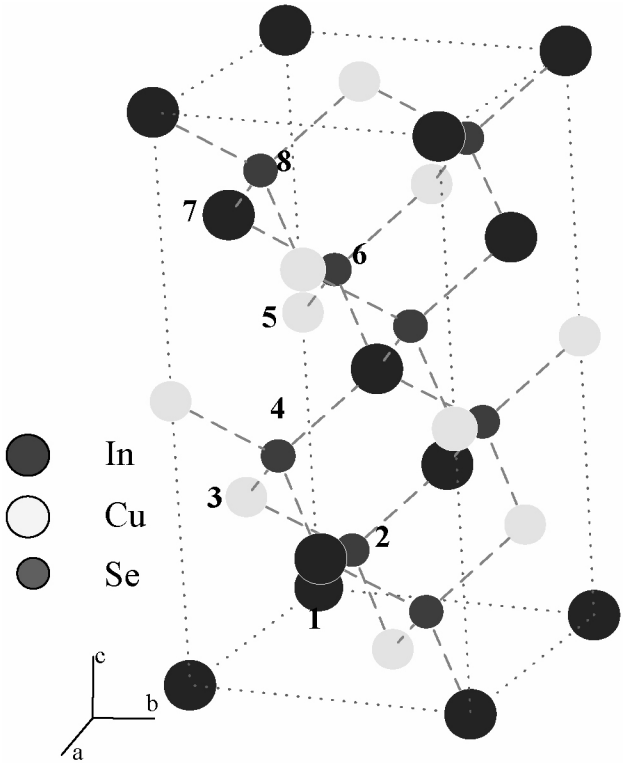

FIGURE 1. Crystal structure for the chalcopyrite CuInM$_2^{VI}$ unit cell.

Chalcopyrites can deviate from their ideal symmetry in two ways. The c/a ratio can be different from its ideal value of 2. This deviation is called tetragonal deformation. Also the anion which lies in the middle of a tetrahedron, can slide along the central axis, which is usually called anionic distortion. In this paper, we present an ideal case, namely, we take $c = 2a$ and the M^{VI} (S, Se, Te) atom at the center of the tetrahedron surrounded by two Cu and two In atoms. We use the tight-binding method. We describe below the way in which we obtained the tight-binding parameters(TBP). They were fitted in such a way that the experimental gap value is reproduced for the whole series. Our Hamiltonians together with the Surface Green's Function Matching (SGFM) method can be used to study surfaces, monolayers, interfaces and superlattices of these materials. In the case of surfaces, a general trend can be formulated only in the ideal case, since within this series, they reconstruct differently in different cases. Reconstruction can be addressed also from the ideal case to compare the different behavior in different cases. The rest of the paper is presented as follows. In Sec. 2, we give some details of the method and of the way in which the TBP are obtained. Section 3 is devoted to some details on how the Hamiltonians were built up. In Sec. 4 we discuss our results in detail, and a short final section contains our conclusions.

2. Some details on the method

We use the tight-binding method [8] to calculate the electronic band structure in the ideal case for the series of chalcopyrites CuInM$_2^{VI}$ with M=S, Se, Te. This method has been used before to describe chalcopyrites successfully [9–13] as well as the related zincblende semiconductor compounds [14, 15]. The method allows the fitting of the experimental gap for the whole series, as we will show below.

In the tight-binding method, Bloch functions $\phi_\upsilon^\mu(\mathbf{k}, \mathbf{r})$ are constructed to describe an electronic orbital υ centered at the position $\tau + \mathbf{d}_\mu$ of the ion labelled μ, as a linear combination of atomic-like orbitals $\psi_\upsilon^\mu(\mathbf{r})$ [8]

$$\phi_\upsilon^\mu(\mathbf{k},r) = \frac{1}{\sqrt{N}} \sum_\tau e^{i\mathbf{k}.(\tau+\mathbf{d}_\mu)} \psi_\nu^\mu(\mathbf{r} - (\tau + \mathbf{d}_\mu)), \quad (1)$$

where $\mathbf{k}$ is a Bloch vector in the First Brillouin Zone and N the number of unit cells in the crystal volume considered. We describe the group III metal In and the group M^{VI} anion with a basis of four atomic-like orbitals of $s-$ and p^3- symmetry. For Cu we consider a full s, p^3, d^5 basis. In chalcopyrite compounds, due to the existence of a tetragonal crystal field and a spin-orbit interaction, the triple degeneracy of the heavy and light hole bands on the top of the valence band presented in zincblende compounds , is lifted. In this work, we only take into account the effect produced by the tetragonal crystal field. The spin-orbit effect is not taken into account in our calculation. The matrix elements of the Hamiltonian have the form:

$$\int \phi_\upsilon^\mu(\mathbf{k}, \mathbf{r}) H \phi_{\upsilon'}^{\mu'}(\mathbf{k}', \mathbf{r}') d\mathbf{r} = \delta_{\mathbf{k},\mathbf{k}'} \sum_{\mathbf{d}_{\mu,\mu'}} e^{i\mathbf{k}.\mathbf{d}_{\mu,\mu'}} \langle \nu | \nu' \rangle_{\mathbf{d}_{\mu,\mu'}} \quad (2)$$

where

$$\langle \nu | \nu' \rangle_{\mathbf{d}_{\mu,\mu'}} = \int \psi_\nu^{\mu*}(\mathbf{r}) H \psi_{\nu'}^{\mu'}(\mathbf{r} - \mathbf{d}_{\mu\mu'}) d\mathbf{r} \equiv V_{\nu\nu'}^{\mu\mu'} \quad (3)$$

and $\mathbf{d}_{\mu\mu'}$ is the position vector of the μ' atom from the μ atom.

A. The tight-binding parameters

To calculate the non-diagonal parameters, $V_{\nu\nu'}^{\mu\mu'}$ in (3), we use Harrison's rule [16]. Therefore the interaction between an atomic-like orbital of symmetry x located at the site $\mu = 1$ (In) with another atom of symmetry y at $\mu' = 2$ (M^{VI}) is

TABLE II. Experimental optical gap for the whole series of Cu-based chalcopyrites considered to set the tight-binding parameters [18].

Chalcopyrite	$E_g^E[eV]$
$CuAlS_2$	3.49
$CuAlSe_2$	2.67
$CuAlTe_2$	2.06
$CuGaS_2$	2.43
$CuGaSe_2$	1.68
$CuGaTe_2$	1.23
$CuInS_2$	1.53
$CuInSe_2$	1.04
$CuInTe_2$	1.02

TABLE III. The on-site tight-binding parameters (in eV) used in the calculation. The parameter $r_\mathbf{d}$ (here in A) is defined in Ref. 16.

Element	Parameter	Harrison	This work
	$E_s[eV]$	-6.92	-14.55
Cu	$E_p[eV]$	-1.83	-2.22
	$E_d[eV]$	-20.14	-16.97
	$r_\mathbf{d}[\AA]$	0.67	1.15
In	$E_s[eV]$	-10.12	-10.12
	$E_p[eV]$	-4.69	-4.69
S	$E_s[eV]$	-20.80	-20.80
	$E_p[eV]$	-10.27	-8.805
Se	$E_s[eV]$	-20.32	-20.32
	$E_p[eV]$	-9.53	-8.789
Te	$E_s[eV]$	-17.11	-17.11
	$E_p[eV]$	-8.59	-8.704

given by $V_{xy}^{12} = lm[V(pp\sigma) - V(pp\pi)]$. To actually calculate the tight-binding parameters, we use further $V(ij\alpha) = \eta(ij\alpha)\hbar^2/md_{\mu\mu'}^2$(and $d_{\mu\mu'}$ is the interatomic distance, m the electron bare mass) for s and p atomic-like orbitals. For the interaction between s, p with d orbitals, we use instead $V(id\alpha) = \eta(id\alpha)\hbar^2 r_d^{3/2}/md_{\mu\mu'}^{7/2}$ (for r_d see Table III and Ref. 16). The $\eta(tw\alpha)$ parameters are given in Ref. 16. If we go on to calculate the diagonal matrix elements using the same procedure, we get an inadmissibly large value for the gap. If we try the tight-binding parameters proposed by Papaconstantopoulos [17] for Cu metal, we do not get the right gap either. Also, the Cu on-site parameters that correctly reproduce the electronic band structure of the superconducting perovskite $YBa_2Cu_3O_7$ fail. Cu orbitals have an important influence on the gap edges in the electronic band structure of the Cu-based chalcopyrites.

In the semiconducting Cu-based chalcopyrites, the s-like orbital plays a major role in fixing the lower edge of the conduction band while the p-like one influences the position of the upper edge of the valence band. The d-like Cu-orbital mostly fixes the value of the chalcopyrite gap. Cu-d orbitals and the p-like C^{VI} ones repel each other and push the upper valence band edge upwards so that the gap is diminished [18–22]. Consequently, we have fixed the Cu on-site parameters for the whole series in such a way that we get the lowest possible deviation from the experimental gap for the whole series of Cu-based chalcopyrites [12]. More precisely, we have selected the three Cu on-site parameters so that $\sum_{series}(E_{series} - E_{gseries}^{E})^2$ as a function of E_{series} is minimal. $E_{gseries}^{E}$ are the experimental values of the gap. Small further adjustments of the anion (M^{VI}) p on-site parameter for each chalcopyrite allowed us to get the right experimental gap for the whole series. The experimental values that we used are quoted in Table II [23].

The on-site tight-binding parameters that we get in this way are compared in Table III to those obtained from Harrison's formulas [16]. Usually, *ab-initio* calculation overestimates the gap and therefore, for an accurate description of the bands around Γ for both the valence and conduction bands, it is convenient to use an approach along the lines that we have followed here. This accurate description of the gap is necessary to further calculate the band structure of surfaces, interfaces and superlattice, which is a goal that we are pursuing.

B. The Hamiltonian

We label the Hamiltonian with the atom numbers as shown below.

	$In1$	$Cu3$	$Cu5$	$In7$	$M^{VI}2$	$M^{VI}4$	$M^{VI}6$	$M^{VI}8$
$In1$	H_{11}	0	0	0	H_{12}	H_{14}	H_{16}	H_{18}
$Cu3$	0	H_{33}	0	0	H_{23}^{+}	H_{34}	H_{36}	H_{38}
$Cu5$	0	0	H_{55}	0	H_{25}^{+}	H_{45}^{+}	H_{56}	H_{58}
$In7$	0	0	0	H_{77}	H_{27}^{+}	H_{47}^{+}	H_{67}^{+}	H_{78}
$M^{VI}2$	H_{12}^{+}	H_{23}	H_{25}	H_{27}	H_{22}	0	0	0
$M^{VI}4$	H_{14}^{+}	H_{34}^{+}	H_{45}	H_{47}	0	H_{44}	0	0
$M^{VI}6$	H_{16}^{+}	H_{36}^{+}	H_{56}^{+}	H_{67}	0	0	H_{66}	0
$M^{VI}8$	H_{18}^{+}	H_{38}^{+}	H_{58}^{+}	H_{78}^{+}	0	0	0	H_{88}

(4)

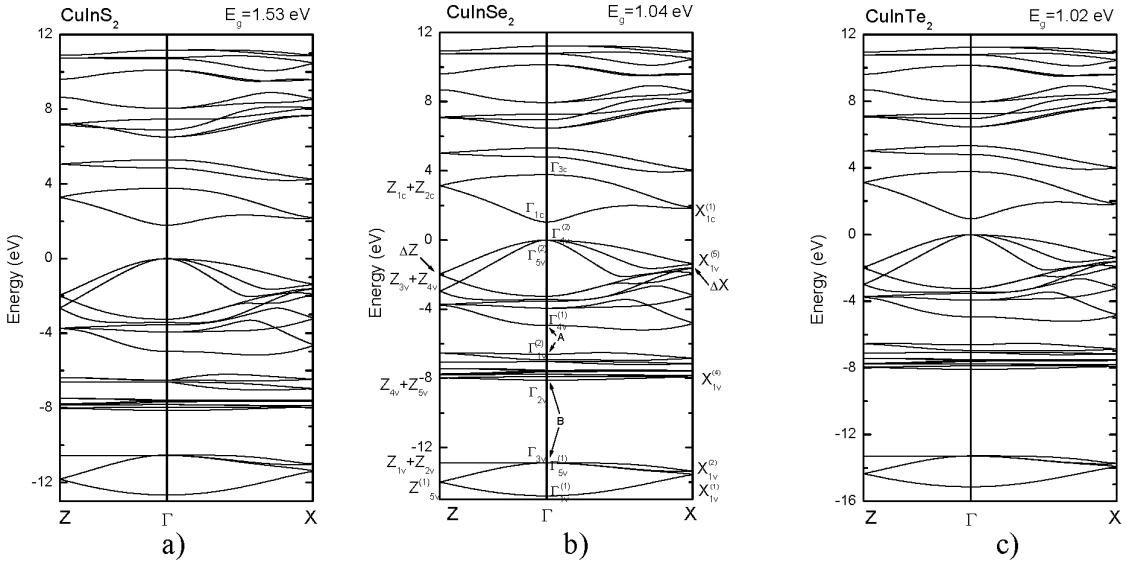

FIGURE 2. The electronic band structure for the series of $CuInM_2^{VI}$ chalcopyrite: a)$CuInS_2$, b)$CuInSe_2$ and c)$CuInTe_2$.

The diagonal sub-matrices are 9×9 for Cu and 4×4 for In and M^{VI}. The Hamiltonian matrix is altogether 42×42.

Obviously, H_{33}=H_{55}. These refer to Cu. H_{11}=H_{77}, on these refer to In. H_{22}=H_{44}=H_{66}=H_{88} which describe the M^{VI} atoms. The non-diagonal sub-matrices describe the first nearest neighbor interactions. Their tight-binding parameters were computed from Harrison's formulas [16], as we already mentioned. We take into account first nearest neighbor interactions only. The anion p-on-site parameter was adjusted further to get the exact experimental gap value in each case. With these data, the Hamiltonian can be built up straightforwardly [25].

3. Results

To get the experimental values for the gaps (see Table II) in our calculated band structure, we made a small (about 8%) further adjustment to the p-on-site parameter for the M^{VI} atom. For example, for $M^{VI} = Se$ the Harrison formula gives 9.53 eV, to be compared with our 8.789 eV. The electronic band structure for the three materials is presented in Fig.2. As in the unit cell of the chalcopyrites, there are two copper atoms that each contribute with six occupied electronic states, two indium atoms, each contributing with three occupied states and four M^{VI} atoms that contribute with two states; therefore, we obtain 26 bands in the valence band. The rest of the 42 bands calculated by the Hamiltonian(16) appear as empty conduction bands, is shown in Fig. 2.

In all the cases presented, both the top valence band of symmetry $\Gamma_{4\nu}^{(2)}$ and the bottom conduction band of symmetry Γ_{1c} are approximately parabolic and therefore in some calculations the free electron effective mass approximation should be a good one. The semiconducting optical gap is direct and is calculated as the difference between the energies Γ_{1c} and $\Gamma_{4\nu}^{(2)}$. The gap values are obtained by fitting them to the experimental ones as we have already remarked (see Table II). These values of the gaps could be accounted for by the optical transitions permitted by symmetry considerations. If the product of the symmetries of the group contains the irreducible representation that corresponds to the dipole (x, y, and/or z), then the transition is allowed, in principle. In our case, the matrix element for dipolar transitions between the top of the valence band and the bottom of the conduction band states at Γ is $\langle\Gamma_{4\nu}^{(2)}|\mathbf{r}|\Gamma_{1c}\rangle$ and is different from zero along the z-axis. The dipole operator for this case which transforms like symmetry Γ_4 , and the product is proportional to the matrix element $\langle\Gamma_{4\nu}^{(2)}|\Gamma_4|\Gamma_{1c}\rangle$ for which $\Gamma_4 \otimes \Gamma_1 = \Gamma_4$ holds, and therefore the transition is permitted.

In general, we observed similar characteristics in the electronic band structure obtained for the whole series.

1. The valence band

Immediately below the singlet state of symmetry $\Gamma_{4\nu}^{(2)}$ (at the top of the valence band), we find a doublet with symmetry $\Gamma_{5\nu}^{(2)}$. The dipolar moment along z is different from zero since the matrix element $\langle\Gamma_{5\nu}|z|\Gamma_{5\nu}\rangle$ is proportional to $\langle\Gamma_5|\Gamma_4|\Gamma_5\rangle$ and satisfies $\Gamma_4 \otimes \Gamma_5 = \Gamma_5$). Therefore the dipolar moment at the top of the valence band (a triplet in the zincblende parent compound) breaks into a zero dipolar moment at the top, $\Gamma_{4\nu}^{(2)}$, and a non-zero one at the doublet, $\Gamma_{5\nu}^{(2)}$. The operator representing the quadrupole moment is proportional to $3z^2 - r^2$, which transforms as Γ_1, and the products of the type $\langle\Gamma_x|\Gamma_1|\Gamma_x\rangle$ are always different from zero since $\Gamma_1 \otimes \Gamma_x = \Gamma_x$, and so a non-zero quadrupole moment will exist for all the valence band states.

The 26 bands that made up the valence band are grouped together into three sub-bands separated by two in-band gaps. The first one (A in Fig.2) separates the upper valence band (UVB) from the middle valence band (MVB) and the in-band gap B separates this band from the lower valence band (LVB). At the top of the UVB there is a singlet, $\Gamma_{4\nu}^{(2)}$, separated from a doublet, $\Gamma_{5\nu}^{(2)}$, by a crystal field splitting, Δ_{cfs}, of about 20 meV for the elements of the series which is zero in the parent zincblende compound, as we mentioned above. Notice that the doublet remains such from $\Gamma - Z$ but splits from $\Gamma - X$.

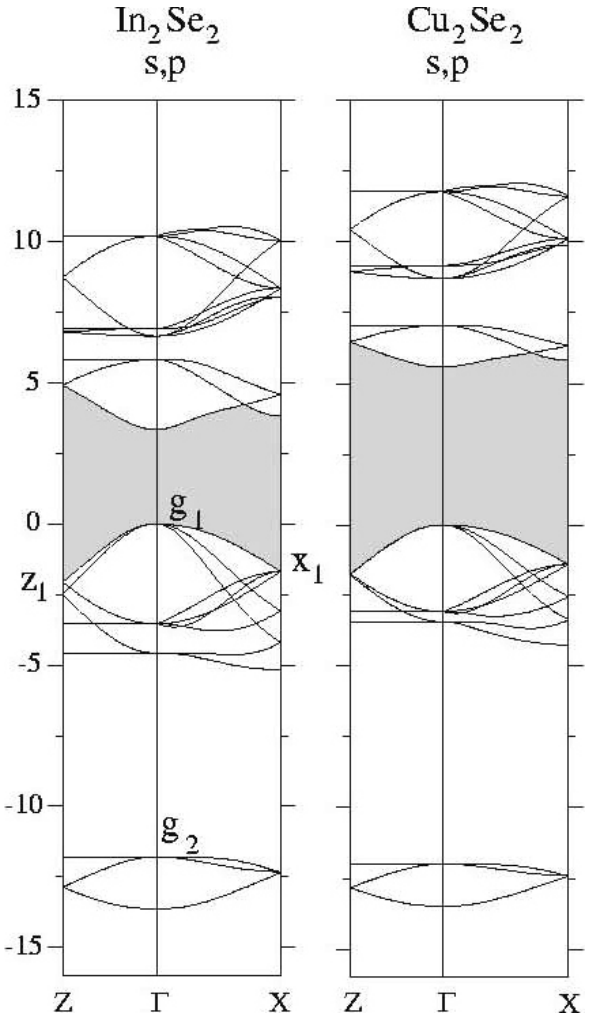

FIGURE 3. The electronic band structure for the hypotetical zincblendes In_2Se_2 and Cu_2Se_2. The three-degeneration folded in Γ reappears by the substitution of the cation symmetry.

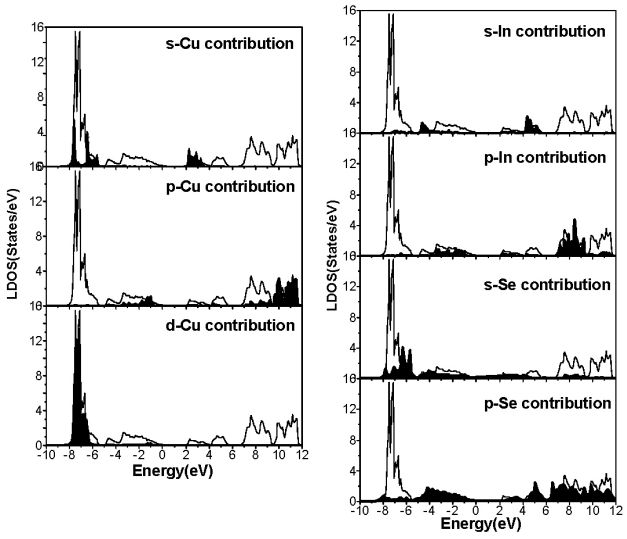

FIGURE 4. Contribution to the DOS from the different orbitals at different energies for the CuInM$_2^{VI}$ chalcopyrite characteristic for the series.

The chalcopyrite crystal field breaks the zincblende symmetry in several ways. First, there are two different cations instead of one, which transforms the symmetry from cubic to tetragonal. Secondly, the anion can be found displaced along the center line of the tetrahedron that it forms together with the two different cations. But the tetragonal symmetry ($c/2a = 1$ where c and a are the lattice parameters) is also broken. We will deal with the effect of these distortions in another work.

a. The upper valence band (UVB)

The splitting of the triplet in the zincblendes into the singlet $\Gamma_{4\nu}^{(2)}$ and the doublet $\Gamma_{5\nu}^{(2)}$ here can easily be found to be due to the presence of the two cations. This can be done with the tight-binding program replacing the parameters for Cu with those of In to get the bands for In$_2$C$_2^{VI}$, or by reversing the way we replace the parameters, we can get Cu$_2$M$_2^{VI}$. In Fig. 3 we present the results for Cu$_2$Se$_2$ and In_2Se_2 for the electronic band structure for the hypotetical zincblendes; in both cases the bands show a triplet on the top of the valence band at Γ. When the bands of the zincblende are compared to those of the chalcopyrite, we realize that two further splittings occur at the top of the valence band, one at Z (ΔZ in Fig. 1) and another one at X (ΔX).

There are 10 bands in the UVB that lie between 0 and -5 eV (the origin is set at the top of the valence band in Γ as is customary). The main contribution comes from three p-like M^{VI} orbitals. The details of the composition are given in Fig.4, where the density of states (DOS) for the CuInSe$_2$ chalcopyrites is shown. It is characteristic for the three members of the series. The shadow areas are proportional to the contribution of the orbital identified in the upper right corner.

b. The middle valence band (MVB)

The inner-band gap A is about 1.6 eV (see Figs. 2 and 4). The MVB contains 12 bands; 10 of them are from the five 3d-Cu orbital contributions. The deepest band of this group runs from $Z_{4\nu} + Z_{5\nu} \rightarrow \Gamma_{4\nu}^{(1)} \rightarrow X_{1\nu}^{(4)}$, as shown in Fig.2.

c. The lowest valence band (LVB)

The deepest group of bands, the LVB, is separated from the MVB by a large gap from $\Gamma_{4\nu}^{(1)}$ to $\Gamma_{3\nu}$ of about 4eV. The main contribution comes from the single $s - M^{VI}$ orbitals (see Fig.4 for more details). The upper band of this group is a singlet $\Gamma_{3\nu}$ followed very closely by a doublet $\Gamma_{5\nu}^{(1)}$. In the zincblende parent compound these bands are degenerate (Fig. 2). This splitting is due to the presence of a second cation. The upper band of this group $Z_{1\nu} + Z_{2\nu} \rightarrow \Gamma_{3\nu}$ is doubly degenerate from $Z - \Gamma$ but splits from $\Gamma - X$.. A comparison of some important values of energy for the high-symmetry points Γ, Z and X are shown in Table IV for the three elements of the series.

2. The conduction band

The conduction band (CB) minimum runs from $Z_{1c} + Z_{2c} \longrightarrow \Gamma_{1c} \longrightarrow X_{1c}^{(1)}$, which is a singlet all along $Z\Gamma X$. At Z, however the band is degenerate, and splits into a higher-in-energy band that runs from $Z_{1c} + Z_{2c} \longrightarrow \Gamma_{3c} \longrightarrow X_{1c}^{(1)}$. At X the band is again degenerate but at Γ_{3c} it is a singlet. From Fig.4, we see that the CB is divided into two clearly defined sub-bands separated by an in-band gap of about 0.2 eV. Each sub-band presents two peaks. The DOS is considerably higher in the upper part of the spectrum. The lowest conduction band (LCB) goes from roughly 1-5 eV. The upper conduction band (UCB) runs from about 5.2-12 eV. The lower peak of the LCB is composed mainly of s-Cu and s-M^{VI} orbitals in the 1-3.7 eV energy region and of s-In and s-M^{VI} in the higher energy region. In the low energy region of the UCB, the main contribution is from p-Cu orbitals and in the higher energy peak it is from p-In ones (see Fig.4 for more details).

A. Comparison with other work

Ab-initio band structure calculations for some chalcopyrites have been made in the past. For CuInS$_2$ and CuInSe$_2$ by Jaffe and Zunger (JZ) [18] and for CuInS$_2$ by Belhaldj *et al.* [24]. To the best of our knowledge there is no calculation for CuInTe$_2$ to compare our results with. It is known that *ab-initio* calculations do not get always the semiconducting gap right. JZ got the values of -0.14 and -0.20 respectively, while Belhardj obtain 0.26 eV. The experimental values are 1.53 and 0.98 eV. Our calculated valence band width ($\Gamma_{4\nu}^{(2)} - \Gamma_{1\nu}^{(1)}$) agrees well for the two materials with both JZ and Belhaldj (see Table IV). The top of the VB, which is a triplet in the zincblende parent crystal structure, splits apart into a singlet

TABLE IV. Comparison between energy values at some high simmetry points taken from Refs. 18 and 24 and our results. For $CuInTe_2$ we did not find any work to compare with.

		$CuInSe_2$		$CuInS_2$		$CuInTe_2$
State	JZ	Belhardj	Ours	JZ	Ours	Ours
UVB-maximum	(eV)	eV	(eV)	(eV)	(eV)	(eV)
$\Gamma_{4v}^{(2)}$	0.00	0.00	0.00	0.00	0.00	0.00
$\Gamma_{5v}^{(2)}$	-0.030	-0.039	-0.02	0.07	-0.01	-0.01
$Z_{3v}+Z_{4v}$	-1.05	-1.009	-1.93	-0.91	-2.19	-1.62
$X_{1v}^{(5)}$	-0.63	-0.52	-1.38	-0.54	-1.54	-1.16
			UVB-minimum			
$\Gamma_{4v}^{(1)}$	-4.66	-5.077	-8.11	-5.07	-8.47	-7.90
$Z_{4v}+Z_{5v}$	-4.61	-4.48	-7.98	-4.90	-8.19	-7.89
$X_{1v}^{(4)}$	-5.02	-5.33	-7.92	-5.41	-8.18	-7.87
s-Se band						
$\Gamma_{5v}^{(1)}$	-13.03	-12.14	-12.91	-13.15	-13.67	-10.08
Γ_{3v}	-13.06	-12.14	-12.90	-13.18	-13.66	-10.06
$\Gamma_{1v}^{(1)}$	-13.83	-13.68	-14.80	-14.57	-15.66	-12.02
$Z_{1v}+Z_{2v}$	-13.00	-12.54	-12.91	-13.18	-13.67	-10.08
Z_{5v}	-13.46	-13.16	-14.00	-13.58	-14.81	-11.23
$X_{1v}^{(2)}$	-13.20	-12.19	-13.36	-13.41	-14.17	-10.47
$X_{1v}^{(1)}$	-13.31	-12.54	-13.57	-13.18	-14.34	-10.85
			Other values			
Width band s-Se at Γ	0.80	1.53	1.90	1.39	2.0	1.96
Gap A	-0.01	1.14	1.67	0.66	1.54	1.60
Gap B	7.39	7.29	4.79	7.1	5.19	2.16
Δz	0.5	-	0.11	no	0.11	0.10
Δx	0.4	-	0.26	no	0.30	0.21
$\Gamma_{5v}^{(1)}-\Gamma_{3v}$	0.03	-	-0.01	-0.03	-0.01	-0.02

at the top and a deeper doublet, a common result in the three works considered. The Δ_{cfs} values for $CuInSe_2$, $\Delta_{cfs}=-0.03$ eV in JZ, and -0.039 in Belhardj are to be compared with our -0.016 eV. This difference shrinks as an effect of the distortions (both anion and tetragonal) which are considered in the *ab-initio* calculations. Yoodee *et al.* [20] have calculated this crystal field splitting $\Delta_{cfs}=0$ for the ideal case, and $\Delta_{cfs}=+0.01$ eV when the tetragonal distortion ($c/a=2.008$) is taken into account. In this case the bands are in a reverse order, which means that the doublet is on the top of the valence band. This can be related to the neglect of the anion distortion. There are some differences in these calculations. We get, in general, a larger value for the width of the UVB (Table IV); for example for $CuInSe_2$, we get 5 eV while JZ get 4 and Belhardj *et al.* get 3 eV. This is actually the origin for the difference in the overall VB width. It is worth mentioning that the inner-band gap A differs substantially in the work by JZ and the other two, even qualitatively. The two bands that define this gap are reverted in JZ's work giving a value of about -0.01 eV while we get a broad inner gap A of about of 1.6 eV that is closer to the 1.14 found by Belhardj et al. The overall width of the MVB does not differ very much in the three works. These differences are shown in detail in Table IV.

4. Conclusions

We have studied the series of Cu-based chalcopyrites CuInM$_2^{VI}$, M^{VI}=S,Se,Te using the tight-binding formalism in order to obtain the electronic band structure. We find that the tight-binding parameters used give an accurate enough result to be useful for further calculations of surfaces, monolayers and interfaces and more complicated systems that include these materials. We also show the effect of the crystal field splitting, calculating the electronic band structure for the hypotetical zincblende In_2Cu_2 and Se_2Cu_2.

1. Y.J. Zhao and A. Zunger, *Phys. Rev. B* **69** (2004) 104422.
2. W.R.L. Lambrecht and S.N. Rashkeev, *J. Phys. and Chem. of Sol.* **64** (2003) 1615.
3. J. Eberhardt *et al. J. Phys. Chem. of Sol.* **64** (2003) 1781.
4. J.A. Muñoz *et al., J. of Appl. Electrochemistry* **28** (1997) 49.
5. I.E. Beckers, U. Fiedeler, S. Siebentritt and M. Ch. Lux-Steiner, *J. Phys. and Chem. of Sol.* **64** (2003) 2031.
6. M. Sugiyama, R. Nakai, H. Nakanishi, and Sf. Chichibu, *J. Phys. Chem of Sol.* **64** (2003) 1787.
7. K. Zweibel, H. S. Ullal, and B. Von Roeden, 26th IEEE Photov. Spec. Conf., Anaheim, CA,(1997) p. 301.
8. J.C. Slater and G.F. Koster, *Phys. Rev.* **94** (1954) 1498.
9. F. Bassani and P. Parravicini, *Electronic States and Optical Transitions in Solids* (Oxford University Press, London, 1975).
10. S. Froyen and W.A. Harrison, *Phys. Rev. B* **20** (1979) 2420.
11. F.A.P. Blom, H. Nachtegaele, and J.T. Devresse, *Phys. Rev. B* **32** (1985) 2334 .
12. J.A. Rodriguez, L. Quiroga, A. Camacho, and R. Baquero, *Phys. Rev. B* **59** (1999) 1555.
13. D. Olguin and R. Baquero, *Eur. Phys. J. B* **32** (2003) 119.
14. D. Olguin and R. Baquero, *Phys. Rev. B* **50** (1994) 1980.
15. D. Olguin and R. Baquero, *Phys. Rev. B* **51** (1995) 16891.
16. W.A. Harrison, *Electronic Structure and the Properties of Solids.* (Dover Publications, Inc. New York, USA 1989).
17. D.A. Papaconstantopoulos, *Handbook of the Band Structure of Elemental Solids.* (Plenum Press, N.Y., 1986).
18. J.E. Jaffe and A. Zunger, *Phys. Rev. B* **28** (1983) 5822.
19. J.E. Jaffe and A. Zunger, *Phys. Rev. B* **29** (1984) 1882.
20. K. Yodee, J.C. Woolley, and S. Yakanit, *Phys. Rev. B* **30** (1984) 5904.
21. S.N. Rashkeev and W.R.L. Lambrecht, *Phys. Rev. B* **63** (2001) 165212.
22. S. Lany and A. Zunger, *Phys. Rev. Lett.* **93** (2004) 156404.
23. J.L. Shay and J.H. Wernick, *Ternary Chalcopyrite Semiconductors.Growth, Electronic Properties and Applications.* (Pergamon Press, Oxford, 1974).
24. M. Belhaldj, A. Tadjer, B. Abbar, Z. Bousahla, B. Bouhafs, and H. Aourag, *phys. stat. sol.(b)* **241** (2004) 2516.
25. J.A. Rodríguez, *Rev. Mex. Fís.* **45** (1999) 584.